

Subzero Osmotic Characteristics of Intact and Disaggregated Hepatocyte Spheroids

B. Korniski,* T. B. Darr,† and A. Hubel*†‡¹

*Department of Biomedical Engineering, Box 368, †Department of Laboratory Medicine and Pathology, Box 609 UMHC, and ‡Biomedical Engineering Center, University of Minnesota, Box 609 UMHC, Minneapolis, Minnesota 55455, U.S.A.

This study has been conducted to examine basic transport characteristics of pig hepatocytes cultured as spheroids for use in a bioartificial liver. Static osmotic experiments were conducted by subjecting hepatocyte spheroids in solutions of increasing sucrose concentrations. A Boyle–van't Hoff plot was used to extrapolate an osmotically inactive volume, V_b , of 0.60, which is unusually high and might not represent the inactive volume of the individual cells. The spheroids were disaggregated and low-temperature cryomicroscopy experiments performed to examine the transport and intracellular ice formation (IIF) characteristics. A hydraulic permeability, L_{pg} , of $7.6 \times 10^{15} \text{ m}^3/\text{Ns}$ and an activation energy, E_{ip} , of 82 kJ/mol was determined for the individual cells. The kinetic (Ω_0) and thermodynamic (κ_0) coefficients for IIF were determined to be $5.9 \times 10^8 \text{ m}^{-2} \text{ s}^{-1}$ and $3.0 \times 10^9 \text{ K}^5$, respectively. These results infer a decrease in the temperature range over which IIF is observed compared to freshly isolated pig hepatocytes. The technique of freeze substitution was used to examine the structure inside the spheroid during freezing. At a low cooling rate of $1^\circ\text{C}/\text{min}$, increasing amounts of intercellular ice formed between the cells. At a higher cooling rate of $100^\circ\text{C}/\text{min}$ small intracellular ice crystals formed. This study shows the location of ice in a freezing hepatocyte spheroid and confirms that the cells cultured as spheroids do not transport water in the same manner as isolated cells. © 1999 Academic Press

Key Words: cryopreservation; spheroid; tissue engineering.

When cultured on positively charged polystyrene (24, 13), modified extracellular matrix molecules (13, 31), or spinner vessels (36), hepatocytes have been observed to form multicellular aggregates roughly spherical in shape referred to henceforth as spheroids. The spheroids are compact structures with extensive cell-to-cell contact and tight junctions (36) which contrasts with aggregates of hepatocytes. The size of the spheroid may vary between 70 and $140 \mu\text{m}$ based on the species of hepatocyte and the method of culture (15, 25, 36). Not all hepatocytes cultured under spheroid-forming conditions become spheroids. Previous studies have shown that roughly 20 to 30% of the isolated hepatocytes cultured will form spheroids (13, 24). When compared to isolated cells,

biotransformation functions are higher in spheroids (16). These attributes indicate that hepatocyte spheroids may be suitable for use in an artificial liver (36, 16).

The clinical and commercial application of hepatocyte spheroids for different tissue engineering applications requires the ability to be cryopreserved. Specifically, cryopreservation would permit pooling of spheroids to reach required cell numbers, completion of safety/sterility testing, and coordination of supply with patient care needs. In a recent study by Lazar and colleagues (16), spheroids cultured in spinner bioreactors maintain urea production synthesis up to approximately 8 days in culture. Albumin synthesis is maintained for longer periods. Recent studies looking at hypothermic storage of hepatocyte spheroids found that spheroid could be stored for up to 3 days at 4°C (28) with comparable levels of biosynthetic function. In clinical applications of a bioartificial liver, determination of the safety of the spheroids may take more than 3 days and, there-

Received February 1, 1999; accepted April 22, 1999.

¹ To whom correspondence should be addressed At Biomedical Engineering Center, University of Minnesota, Box 609 UMHC, Minneapolis, MN 55455. Fax: (612) 625-1121. E-mail: hubel001@maroon.tc.umn.edu.



fore, frozen storage of the spheroids would be desirable.

The post-freeze-thaw survival of cells depends upon a variety of factors. During freezing, solute is rejected from the solid phase producing an abrupt change in concentration in the unfrozen portion of solution. A cell responds to this perturbation by expressing water to reach a new equilibrium state between intracellular and extracellular solutions. At high cooling rates, equilibrium cannot be maintained because the rate at which the chemical potential in the extracellular solution is being lowered is much greater than the rate at which water can diffuse out of the cell (14). The end result of this imbalance is that intracellular ice formation (IIF) is observed which is lethal to the cell (cf. Ref. 32 for review). At low cooling rates, cells are exposed for long periods of time to high extracellular concentrations resulting in potentially damaging high intracellular concentrations (18, 23). Mechanical stresses during slow freezing are also felt to contribute to damage (11, 20).

Organized tissues have a three-dimensional structure that requires additional considerations with regard to cryopreservation. Multicellular tissues contain multiple cell types, extracellular matrix, and other structures such as blood vessels. The heterogeneity in composition and structure combined with limitations in heat and mass transfer result in distinct differences in freezing environment experienced by individual cells embedded in the tissue during freezing. The surface area available for mass transfer is also determined by the tissue organizational structure and the extracellular volumes (27). All of these influences affect the viability and distribution of viabilities within a tissue that is cryopreserved.

The water content and flux of water are a central element to the description of the biological response of a cell (or spheroid) to the freeze-thaw process. The overall objective of this investigation is to determine experimentally the basic osmotic response of the hepatocyte spheroid. Specifically, the osmotic response of the spheroid to hypertonic stresses present at sub- and

suprazero temperatures will be determined. This information will be essential in understanding the flow of water in a multicellular system and the development of appropriate preservation protocols for hepatocyte spheroids.

METHODS

Cell Isolation and Spheroid Culture

Pig hepatocytes were harvested from 8- to 10-kg male pigs using a two-step *in situ* collagenase perfusion technique that was modified from the original method developed by Seglen (29). The pig was initially anesthetized with ketamine and rompun to allow for intubation and mechanical ventilation and subsequently anesthetized with isoflurane and paralyzed with succinylcholine. The liver was first perfused *in vivo* with oxygenated perfusion solution I (Per I) at 300 ml/min for 20 to 40 min. Per I is a calcium-free solution with 143 mM sodium chloride, 6.7 mM potassium chloride, 10 mM Hepes (Gibco, Grand Island, NY), and 1 g/L EDTA (Sigma Chemical Co., St. Louis, MO) at pH 7.4. The liver was then perfused *ex vivo* at 300 ml/min with oxygenated perfusion solution II (Per II). Per II consists of 100 mM Hepes, 67 mM sodium chloride, 6.7 mM potassium chloride, 4.8 mM calcium chloride, 1% (v/v) bovine albumin, and 1 g/L collagenase-D (Sigma), pH 7.6. Once the liver was visually dissolved (after 20–30 min), it was broken up and irrigated with cold William's E medium (Gibco) supplemented with 15 mM Hepes, 0.2 U/ml insulin (Lilly), 2 mM L-glutamine (Gibco), 100 U/ml penicillin (Celox, Hopkins, MN), and 100 mg/ml streptomycin (Celox). The released cells were filtered through nylon mesh with 100- μ m openings and washed via three centrifugations (50 g) and resuspensions in the William's E medium. Viability for the harvests as determined using trypan blue exclusion ranged from 89 to 98%.

Culture of Hepatocyte Spheroids

Hepatocyte spheroids were formed in spinner vessel culture using technique described in more detail in Ref. (15). Briefly, isolated hepa-

toocytes were inoculated into a spinner flask containing 100 ml of medium to a final concentration of 3×10^5 viable cells per milliliter. The medium consisted of William's E medium (Gibco, Grand Island, NY) containing 0.292 mg/ml L-glutamine (Gibco), 0.2 U/ml of porcine insulin (Lilly Research Laboratories, Indianapolis, IN), 25 ng/ml of epidermal growth factor, 50 g/ml linoleic acid, 500 mg/ml bovine serum albumin, 1 nM dexamethasone, 4 ng/ml glucagon, 6.25 mg/ml transferrin, 20 ng/ml of liver growth factor, 6.25 ng/ml of selenium, 0.1 mM $\text{CuSO}_4 \cdot 5\text{H}_2\text{O}$, 3 nM H_2SeO_3 , 50 pM $\text{ZnSO}_4 \cdot 7\text{H}_2\text{O}$, 15 mM HEPES, 100 U/ml penicillin (Celox, Hopkins, MN), 100 mg/ml of streptomycin (Celox). All components were from Sigma unless otherwise indicated. The flask was cultured in a 37°C incubator with 5% CO_2 while being stirred using a magnetic stirring plate set at a speed of 90 rpm. Spheroid formation was complete approximately 48 h after inoculation of the isolated cells into the spinner flask. The spheroids could be maintained in the spinner flasks for several weeks with medium changes every 2–3 days.

Cryomicroscopy System

The controlled freezing experiments were performed using a cryomicroscope (cf. 4) which consisted of a Zeiss general research microscope (Carl Zeiss, FRG) fitted with a specially designed cryostage described in detail elsewhere (4). Images from the light microscope were transmitted to a video cassette recorder (JVC HR-S6900U) and a color monitor (Sony PVM 1344Q) by a camera (Optronics LX450A) to allow direct visual observation and recording of the freezing experiments. A computer-based temperature controller and video interface (Thermascope and Datavideo, Interface Techniques, Cambridge, MA) was used to specify and control the stage temperature. A 10× bright-field objective (Carl Zeiss) combined with a 2× optovar (Carl Zeiss) was used for magnification of the experiments. The freezing studies were performed on a thin convection stage. The experimental sample was placed on a composite window consisting of an optically

transparent heating layer made of indium tin oxide, a thermocouple for sensing temperature, and a sapphire substrate designed to isolate the thermocouple from the freezing solution and reduce temperature gradients. Gaseous nitrogen, chilled in a bath of liquid nitrogen, provided refrigeration for the cryostage. Stage temperature during experiments was regulated by the Tempsoft software (Interface Techniques) which controlled the amount of power to the heating layer. For a freezing experiment, a 3- to 5- μl sample of the cell suspension, or a 25- μl sample of spheroid suspension, was placed between the cryostage window and a glass coverslip. The sample was cooled from room temperature to a holding temperature, typically -2°C , where a chilled probe was used to seed ice formation in the extracellular solution. Immediately after seeding, the sample was cooled at a low constant rate to a final temperature of -10 to -20°C , depending on the cooling rate. For the determination of IIF parameters, samples were instead cooled at $100^\circ\text{C}/\text{min}$ to -40°C . The stage was then warmed to room temperature and the sample was removed. Due to difficulties in recovering the sample, the cells frozen using the cryomicroscopy system could not be tested postthaw for viability.

Osmotically Inactive Volume of Spheroid

The total water content of the cells in the spheroid consists of the water available for transport and the osmotically inactive water. The osmotically inactive volume of the spheroids was obtained by placing a sample of spheroids into hypertonic solutions of increasing osmolarity (300–1000 mOsm). The hypertonic solutions were made by adding sucrose to William's E medium. In order to reduce the experimental scatter, a specific spheroid was placed in each of the solutions tested. After equilibration, the static volume of the spheroids was determined using image analysis. The cross-sectional area of the spheroid was measured for each concentration and converted to a volume assuming that the spheroid was spherical. For each experiment, at least eight spheroids were followed through the different concentrations of sucrose solutions.

Disaggregation of Spheroids

Previous studies have shown that *ex vivo* cultured hepatocytes can exhibit differences in water transport characteristics (37). In order to obtain an estimate for the water transport characteristics of the cells in the spheroid, a small number of spheroids were disaggregated and the freezing characteristics of the hepatocytes isolated from the spheroid were determined using cryomicroscopy. Small aggregated and isolated cells were removed by filtration of the samples through a 40- μm nylon mesh (Falcon, Franklin Lakes, NJ). The spheroids larger than 40 μm in diameter are placed in trypsin-EDTA (Gibco) solution and agitated with a pipette every 5 min. After 15 to 20 min, the spheroids were mostly disaggregated into isolated cells with a minority of cells joined to form couplets and triplets. The solution was diluted with an equal volume of culture medium and then centrifuged at 70g in a Marathon 6K centrifuge (Fisher Scientific, Hampton, NH) for 10 min. The supernatant was discarded and the cells were resuspended in William's E medium.

Freeze Substitution of Spheroids

In order to determine the osmotic behavior of spheroids in the presence of external ice, hepatocyte spheroids were frozen at a controlled cooling rate on the cryomicroscope stage and then freeze-substituted and sectioned. A 25- μL volume of hepatocyte spheroids and culture medium was placed on a piece of 40- μm mesh resting on the cryomicroscope stage. The samples were cooled at a controlled rate (100 and 1°C/min) to a specified final temperature (between -3 and -60°C). Using prechilled forceps, the mesh and cooled spheroids were removed from the cryomicroscope stage and plunge-frozen in a tray of liquid nitrogen. As controls, spheroid samples at room temperature were also plunge-frozen in the same manner without the controlled-rate freezing on the cryomicroscope stage.

In order to permit determination of the ice crystal structure inside the spheroid during the freezing process, the ice in the frozen hepatocyte spheroid samples was removed using a process of freeze substitution (cf. Ref. 26 for more details).

Specifically, each sample containing a piece of nylon mesh and several spheroids was placed in 1 ml of a solution 2 g OsO_4 /100 ml acetone at -90°C. The samples were then held at -90°C for 24 h, -60°C for 2 h, -30°C for 2 h, and 0°C for 30 min and then equilibrated to room temperature in a FSU 010 freeze substitution device (Balzers, Liechtenstein). The osmium/acetone medium was removed from the ice-substituted spheroid samples and replaced with 100% acetone. The samples were washed at room temperature three times with acetone, twice with a 1:1 acetone:Quetol mixture, and twice with pure Quetol (Electron Microscopy Sciences, Ft. Washington, PA) in order to impregnate the freeze-substituted material. The sample embedded with Quetol was polymerized in an oven for 12 h at 70°C and then sectioned to 0.5 μm thickness on a Mark 2 Huxley-Pattern Ultramicrotome (LKB, Sweden). The sections were mounted on microslides heated on a hot plate and stained with toluidine blue. A similar protocol was used by Pazhaynur and colleagues (1997) to determine dehydration in intact tissues.

Water Transport Model

The dehydration observed during the freezing of isolated cells obtained from disaggregated spheroids performed using a cryomicroscope was analyzed to determine the water transport characteristics of those cells. During freezing, the efflux of water was assumed to result from an imbalance in the chemical potential between intracellular and extracellular solution. Using a nonequilibrium thermodynamic model developed by Mazur (19), the following equation can be written

$$\frac{dV}{dT} = \frac{L_p A R T}{\nu_w B} \left[\ln \left(\frac{V - V_b}{(V - V_b) + \nu_w (\nu_s n_s)} \right) - \frac{\Delta H_f}{R} \left(\frac{1}{T_R} - \frac{1}{T} \right) \right], \quad [1]$$

where V is the cell volume, T is the temperature (absolute), L_p is the hydraulic permeability, A is the surface area of the cell, B is the cooling rate, ν_w is the partial molar volume of water, n_s is the number of moles of salt in the cell, ν_s is the dissociation constant for NaCl, V_b is the osmotically inactive cell volume fraction, T_R is the

equilibrium freezing temperature for pure water (273.15 K), and ΔH_f is the latent heat of fusion of water. This equation is based on the assumption that equilibria of temperature and pressure prevail between the intra- and extracellular media. Furthermore, the permeability of the membrane is rate limited by the passage of water through the cell membrane. Assuming an Arrhenius relationship (17, 34), the permeability is expressed as a function of temperature

$$L_p = L_{pg} \exp\left(-\frac{E_{lp}}{R} \left(\frac{1}{T} - \frac{1}{T_R}\right)\right), \quad [2]$$

where L_{pg} is the permeability of the cell membrane to water at the reference temperature, T_R , and E_{lp} is the apparent activation energy for the water transport process.

Implicit within the development of these equations is the assumption that thermal equilibrium exists within the immediate region around the cell and the temperature difference across the cell membrane is less than 0.01°C . The intracellular solution is assumed to be ideal and dilute. As with most mammalian cells, it is assumed that the hydrostatic or turgor pressure across the cell membrane is negligible. A more complete discussion of the assumptions behind this model and the errors associated with these can be found elsewhere (34).

Intracellular Ice Formation Model

There is evidence that high cooling rates result in excessive supercooling and concomitantly intracellular ice formation (32). Models have been developed to predict ice formation in biological cells. The disaggregated cells have been characterized according to a model based on heterogeneous nucleation theory (33). The rate of heterogeneous ice formation, J_{het} , can be written as

$$J_{het} = \Omega_o \frac{\eta_o}{\eta} \left[\frac{T}{T_{fo}}\right]^{1/2} \exp\left[\frac{-\kappa_o}{\Delta T^2 T^3} \left(\frac{T_f}{T_{fo}}\right)^4\right] \quad [3]$$

and the probability of ice formation is

$$PIF = 1 - \exp\left[-\frac{1}{B} \int_{T_{seed}}^T A J_{het} dt\right], \quad [4]$$

where the subscript 'o' refers to isotonic conditions. The respective kinetic (Ω_o) and thermodynamic (κ_o) parameters for nucleation can be determined as a function of the specific cell type. Additionally, η is the viscosity, T_f is the equilibrium freezing temperature of the cell cytoplasm, ΔT is the supercooling, and A is the surface area for nucleation.

Data Analysis

The dehydration of the isolated cells observed in the cryomicroscopy experiments was analyzed to provide an estimate of the water transport from each cell. The corresponding image analysis was done on a Apple Power Macintosh 7600/132 computer (Apple, Cupertino, CA) using NIH Image processing software (U.S. National Institutes of Health). Images obtained at specific time points were digitized from the videotape and analyzed. A cursor was used to trace the outline of the cell boundary and the enclosed area was calculated and entered into a spreadsheet that included other information such as the temperature. The cross-sectional area of the cell was related to the cell volume assuming spherical geometry. For each cooling rate, cell volumes were obtained at approximately 10 different temperatures and for the same experimental conditions at least eight cells were analyzed.

As indicated previously, the hydraulic permeability, L_{pg} , and its temperature dependence, E_{lp} , can be estimated based on the experimental measurements of cell area as a function of time/temperature using the previously described model. The inverse curve-fitting method used to relate the experimental measurements to the models uses nonlinear regression analysis to produce the permeability values that would yield the best fit between experimental volume measurements and theoretical volumes with the criteria of minimizing the χ^2 (17). The values of L_{pg} and E_{lp} can in turn be used to predict water transport and content for an arbitrary freezing protocol.

Microscopic sections of the freeze-substituted spheroids were examined an Olympus BH-2 light microscope (Olympus America Inc.,

Melville, NY) instrumented with a SPOT digital camera (Diagnostic Instruments Inc., Sterling Heights, MI). Digital images from the camera were sent directly to a Micron Powerdigm XSU computer (Micron Technology Inc., Boise, ID). After the completion of the staining process, the cells are denoted as dark blue and the remaining space that contained ice crystals prior to the substitution process would be light/transparent. Subsequent image preparation of the pictures was performed using Adobe Photoshop (Adobe Systems Inc., San Jose, CA) before analysis. The blue portions of the images were selected and copied to a blank background so that the image would only contain the cellular material and the uniform background. The image analysis of the spheroids was done using NIH Image by placing a threshold on the color intensity and calculating the image area above the set threshold.

For the freeze-substitution experiments, the fraction of cellular area of the section was used to estimate the dehydration as a function of final temperature. In order to compare the dehydration from the spheroid initial state, this fraction was normalized over the initial cell area to spheroid fraction from the samples plunged at room temperature. Furthermore, if the sectioned samples are representative throughout the entire depth of the spheroids, then any incremental unit depth (Δz) multiplied by the areas would approximate a volume. A volume fraction calculated by this assumption would be the same as the area fraction. The normalized fraction of cells was calculated from the cross-sectional areas,

$$\text{Normalized Fraction} = \frac{A_{\text{Cells}}/A_{\text{Spheroid}}}{A_{i,\text{Cells}}/A_{i,\text{Spheroid}}} \quad [5]$$

and this is comparable to a volume calculation by assuming an incremental depth to the measurements,

$$\frac{A_{\text{Cells}}}{A_{\text{Spheroid}}} \frac{\Delta z}{\Delta z} = \frac{V_{\text{Cells}}}{V_{\text{Spheroid}}} \quad [6]$$

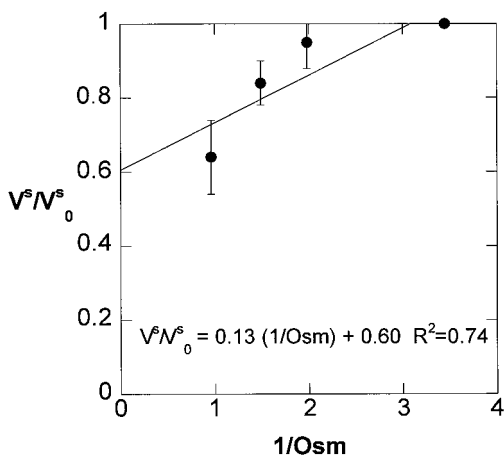


FIG. 1. Normalized spheroid volume fraction, V/V_0 , as a function of the inverse of solution osmolarity for pig hepatocyte spheroids. Error bars indicate standard deviation of the mean. Linear regression was used to determine the Boyle–van’t Hoff relationship for the data represented in these figures.

RESULTS

Osmotic Response at Suprazero Temperatures

The first phase of the investigation involved a determination of the spheroid osmotic response at suprazero temperatures. The osmotically inactive spheroid volume fraction was determined based on the equilibrium volume of the spheroid in hypertonic solutions of increasing concentration. A Boyle–van’t Hoff plot, the normalized spheroid volume (volume at a given concentration divided by the volume under isotonic conditions) as a function of the inverse of solution osmolarity, is given in Fig. 1 for pig hepatocyte spheroids. Extrapolating to infinite concentration, the osmotically inactive spheroid volume fraction for the cell was determined to be 0.60.

Cryomicroscopy of Hepatocytes Disaggregated from Spheroids

The increase in concentration of the extracellular solution during freezing results in a decrease in the cell volume as a function of temperature for a given cooling rate. The dehydration of pig hepatocytes isolated from spheroids for a constant cooling rate of $1^\circ\text{C}/\text{min}$ is given in Fig. 2A. Based on the decrease in

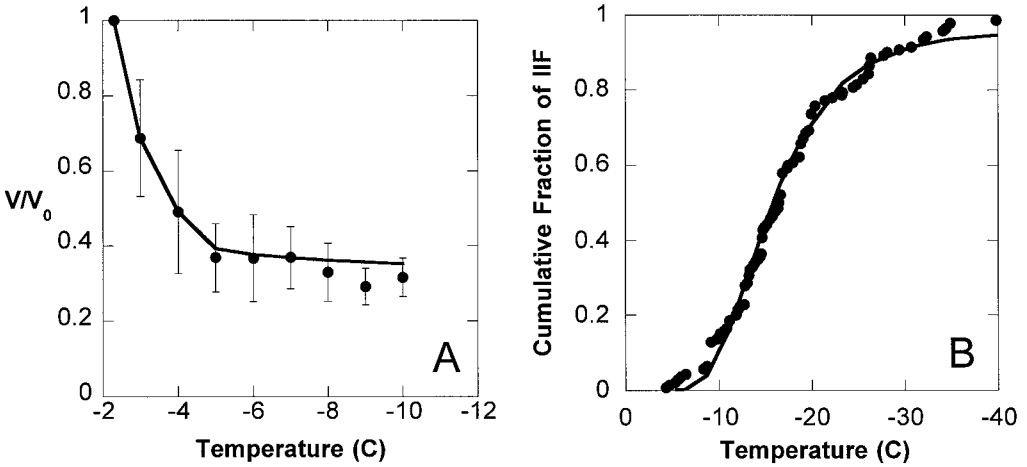


FIG. 2. Cryomicroscopy data and model correlation for cells that were disaggregated pig hepatocyte spheroids. Points are the experimental data and lines are the best fit for the model Eqs. [1]–[4]. (A) Normalized cell volume fraction, V/V_o , as a function of temperature. The cells were frozen in William's E medium at a cooling rate of $1^\circ\text{C}/\text{min}$. Error bars indicate standard deviation of the means. A total of 8 cells were analyzed in these experiments. (B) Cumulative fraction of intracellular ice formation as a function of temperature. 70 cells were frozen at $100^\circ\text{C}/\text{min}$.

cell volume obtained using image analysis, estimates for the hydraulic permeability, L_{pg} and activation energy, E_{ip} were obtained for cooling rates of 1, 3, and $5^\circ\text{C}/\text{min}$ (Table 1). The average value for the reference water permeability, L_{pg} , was determined to be $0.76 \pm 0.51 \times 10^{-14} \text{ m}^3/\text{Ns}$ and the activation energy, E_{ip} , was $82 \pm 63 \text{ kJ/mol}$. The average cell diameter was $22.09 \pm 2.25 \mu\text{m}$. A minimum volume fraction of the disaggregated cells was found to be 0.32 when cooled at $1^\circ\text{C}/\text{min}$. This value was assumed to be the osmotically inactive volume

fraction, V_b , used in the subsequent theoretical analysis. Static osmotic experiments were performed on the disaggregated hepatocyte spheroids. Exposure to hypertonic solutions resulted in extensive cell blebbing and death even for short periods of exposure.

The ability to predict the probability of IIF requires the experimental determination of the ice nucleation parameters, Ω_o and κ_o . If the cooling rate used is sufficiently high to suppress water transport out of the cell, the cumulative fraction of cells as a function of temperature can

TABLE 1
Water Transport Characteristics for Disaggregated Pig Hepatocyte Spheroids Obtained Using Cryomicroscopy at Different Cooling Rates

B ($^\circ\text{C}/\text{min}$)	L_{pg} (m^3/Ns)	E_{ip} (kJ/mol)	Cell diameter (μm)	V_{min}^a	χ^2	No. of cells
1	6.329×10^{-15}	60.84	19.53	0.316	1.02×10^{-3}	8
3	3.281×10^{-15}	31.98	23.71	0.441	6.21×10^{-3}	11
5	1.314×10^{-14}	152.6	23.04	0.391	3.60×10^{-4}	10
Avg.	7.583×10^{-15}	81.81	22.09	0.383		
SD	5.048×10^{-15}	62.98	2.25	0.063		

^a Minimum volume fraction for the cells during a specific experiment.

be used to estimate the values of the IIF parameters. For a cooling rate of $100^{\circ}\text{C}/\text{min}$, the cumulative fraction of cells with IIF as a function of temperature for disaggregated pig hepatocyte spheroids is given (Fig. 2B). The fraction of cells with IIF increases with decreasing temperature. The experimentally determined kinetics were then correlated with Eqs. [3] and [4] to obtain the nucleation parameters, Ω and κ , which were $5.9 \times 10^8 \text{ m}^{-2} \text{ s}^{-1}$ and $3.0 \times 10^9 \text{ K}^5$, respectively.

Osmotic Response at Subzero Temperatures

Previous studies of rat hepatocyte spheroids showed that there was little change in the outer diameter of a spheroid during conventional cryomicroscopy (5). Ultrastructural studies of hepatocyte spheroids had shown the existence of bile-cannaliculi-like structures between adjacent hepatocytes in the spheroids (15). The next phase of the investigation focused on determining the internal structure of the spheroid during freezing. Specifically, the cell volume and location of ice crystals as a function of final temperature and cooling rate was investigated. These studies would help determine the role of the bile-cannaliculi-like structures in the freezing response of spheroids.

In a series of control experiments, spheroids were taken out of culture and plunged into liquid nitrogen. It is assumed that the cooling rate for these experiments was sufficiently high to suppress water transport and the sections resulting from the freeze substitution represent the normal internal structure of the spheroid. A photomicrograph of one of the internal structure of the spheroid is shown in Fig. 3. The cells are seen to be compact with very little extracellular area between the cells. The darkest regions of the spheroid correspond to the cytoplasm. Lighter regions correspond to the nucleus of the cells. A light region between two adjacent cells that may correspond to a bile-cannaliculi-like structure is denoted with an arrow. The method of freeze substitution did not result in visible ice crystals at this level of magnification for this sample.

When the spheroid was cooled rapidly

($100^{\circ}\text{C}/\text{min}$) to a final temperature of -60°C , small but visible ice crystals (denoted by an arrow) are present in the spheroid (Fig. 4). The ice crystals are found more commonly in the center of the spheroid and the diameter of the crystals is typically less than $22 \mu\text{m}$ cell diameter. If the cooling rate was reduced, distinct changes in the internal structure of the hepatocyte spheroid are observed during cooling. In Fig. 5, freeze-substituted sections of spheroids cooled at $1^{\circ}\text{C}/\text{min}$ to a final temperature of -3 , -5 , -12 , or -16°C is given. At -3 and -5°C , small ice crystals are visible and slight dehydration of the cells in the interior of the spheroids is observed. As the final temperature is decreased to -12 and -16°C , the average size of the visible ice crystals increases and dehydration of the cells is more prominent.

Using image analysis, the normalized fraction of cell volume was determined as a function of temperature for a cooling rate of $1^{\circ}\text{C}/\text{min}$ (Fig. 6). The normalized fraction of cell volume represents the ratio of cellular area at a given temperature, T , divided by the overall cross-sectional area of the spheroid (cf. Eqs. [5] and [6]). This parameter reflects the dehydration of the cells comprising the spheroid. The normalized fraction of cell volume in the spheroids decreases with decreasing temperature to value of 0.52 by -16°C . Not surprisingly, the dehydration of hepatocytes in intact spheroids is significantly less than that observed in hepatocytes disaggregated from spheroids frozen under the same conditions (cf. Fig. 2A).

DISCUSSION

The osmotic response of hepatocyte spheroids is an important characteristic of its freezing behavior. It is clear based on the observations in this investigation that the osmotic response of spheroids is more complex than that of isolated cells. Although little change in outer diameter was observed during the freezing of spheroids using cryomicroscopy, significant changes in spheroid volume were observed when the spheroids were exposed to hypertonic solutions at suprazero temperatures. The osmotically inactive cell volume fraction of pig hepa-

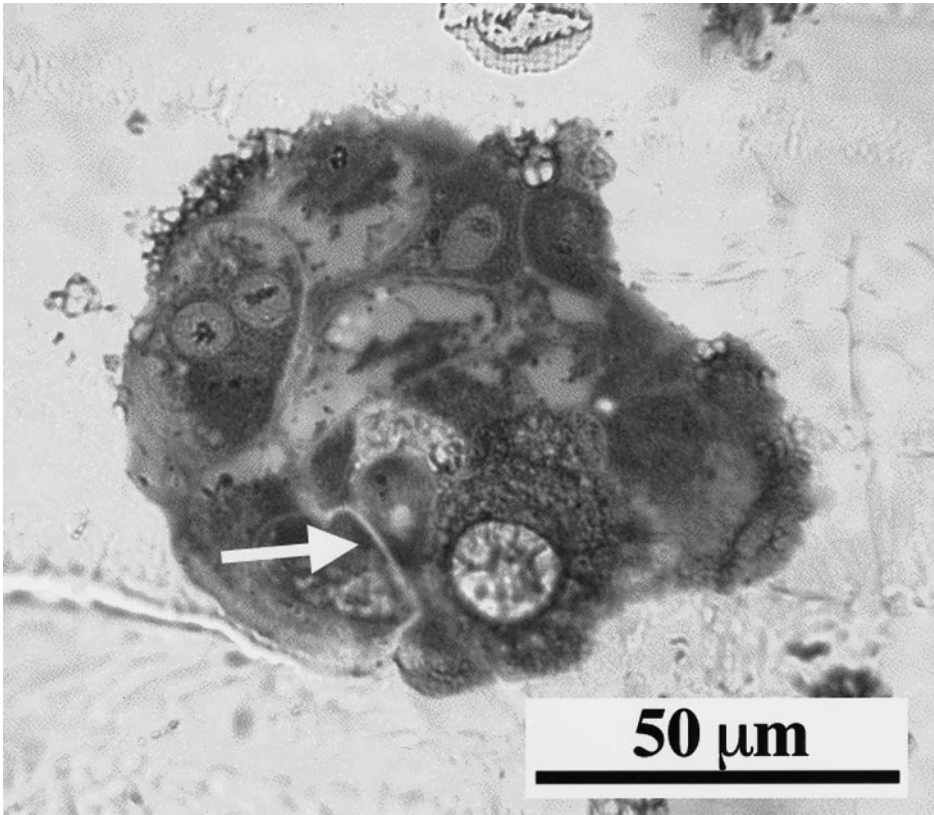


FIG. 3. Cross-sectional slice of a hepatocyte spheroid that was plunge frozen from room temperature and freeze substituted. The internal structure of the spheroid can be observed with cell nuclei and internal structures resolved.

toocyte spheroids (0.60) was much higher than the value measured previously for freshly isolated pig hepatocytes (0.25, from Ref. 6) and pig hepatocytes obtained from disaggregated spheroids using in this investigation (0.32). The linear fit of the data obtained from the Boyle-van't Hoff has a rather poor value for r^2 (0.74), which indicates that pig hepatocyte spheroids may not act as perfect osmometers. Similar studies performed using rat hepatocyte spheroids showed a more linear relationship than that observed using pig hepatocytes (data not shown) and it is not clear whether the differences reflect experimental error or species-related differences in osmotic properties.

When cultured to form spheroids and then disaggregated, the values of L_{pg} and E_{ip} for pig hepatocytes decrease significantly from the val-

ues obtained from freshly isolated pig hepatocytes (cf. Table 2). This change in water permeability parameters was consistent with the decrease in L_{pg} and E_{ip} observed previously with isolated rat hepatocytes and rat hepatocytes cultured in a collagen gel (37). Differences in water permeability and IIF characteristics after *in vitro* culture of hepatocytes may, in turn, influence the selection of optimal freezing conditions for cultured versus freshly isolated hepatocytes. Difference in culture conditions (i.e., culture in a collagen gel or cultured to form spheroids) may also influence the freezing conditions required. The difficulty in determining the osmotically inactive cell volume fraction for disaggregated hepatocyte spheroids observed in this investigation is consistent with previous studies of the water transport characteristics for

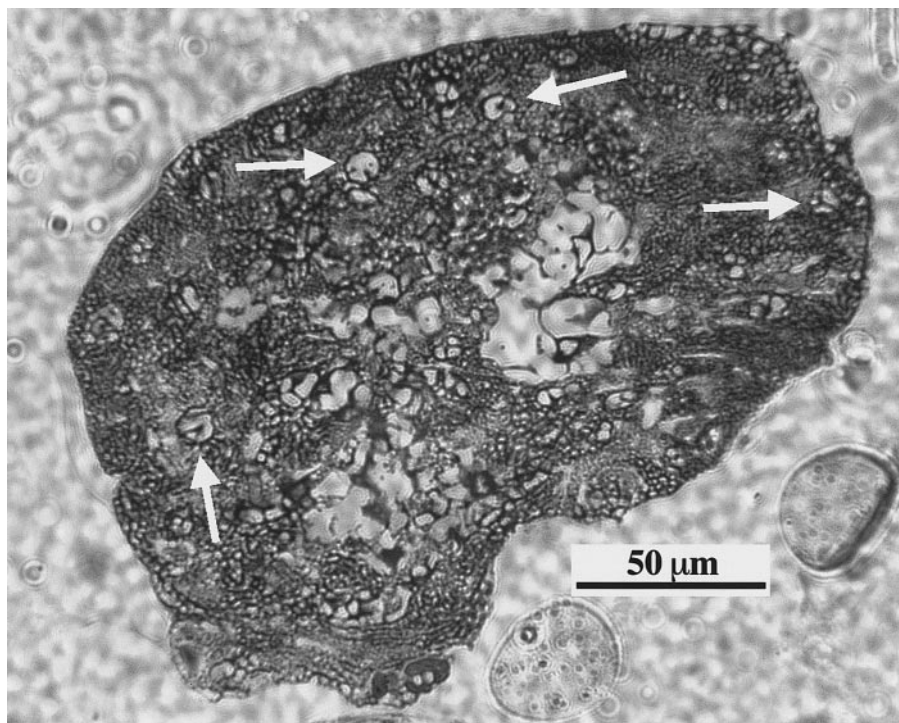


FIG. 4. Cross-sectional slice of hepatocyte spheroid that was frozen at $100^{\circ}\text{C}/\text{min}$ to a final temperature of -60°C . The dark regions denote hepatocytes. Light regions indicate the location of fine ice crystals present inside cells comprising the spheroid. The arrows indicate regions of intracellular ice formation.

freshly isolated hepatocytes (6, 34). As a result, osmotically inactive cell volume fractions for hepatocytes are typically determined from dehydration characteristics at subzero temperatures.

The culture of hepatocytes to form spheroids also influenced the IIF characteristics of the cells. The temperature at which 50% of the cells formed IIF for a cooling rate of $100^{\circ}\text{C}/\text{min}$ decreased approximately 9°C when hepatocytes were cultured to form spheroids and then disaggregated (when compared to freshly isolated pig hepatocytes (6)). The formation of IIF at relatively high subzero temperatures represents a significant obstacle to the cryopreservation of isolated hepatocytes (12). The specific mechanism responsible for the significant decrease in the temperature over which IIF was observed for the cultured hepatocytes was not determined in this investigation. The potential exists that cultured hepatocytes could be used as an appro-

priate model to investigate the potential nucleating sites for IIF.

As indicated in the freeze-substitution studies, the dehydration characteristics of hepatocyte spheroids differ from hepatocytes disaggregated from spheroids and freshly isolated pig hepatocytes (6). This finding is consistent with previous studies in which water transport parameters of rat liver tissue were determined. The water transport values for rat liver tissue by freeze substitution microscopy were $L_{pg} = 3.1 \times 10^{-13} \text{ m}^3/\text{Ns}$, $E_{ip} = 290 \text{ kJ/mol}$, and $V_b = 0.35$ (22) which differs from the values obtained for isolated rat cells (cf. Table 2). Further study is needed to determine the mechanism responsible for the changes in permeability observed with different culture conditions.

The freeze-substitution analysis of hepatocyte spheroids was important in characterizing both the dehydration of the cells in the spheroid and the distribution of ice throughout the spher-

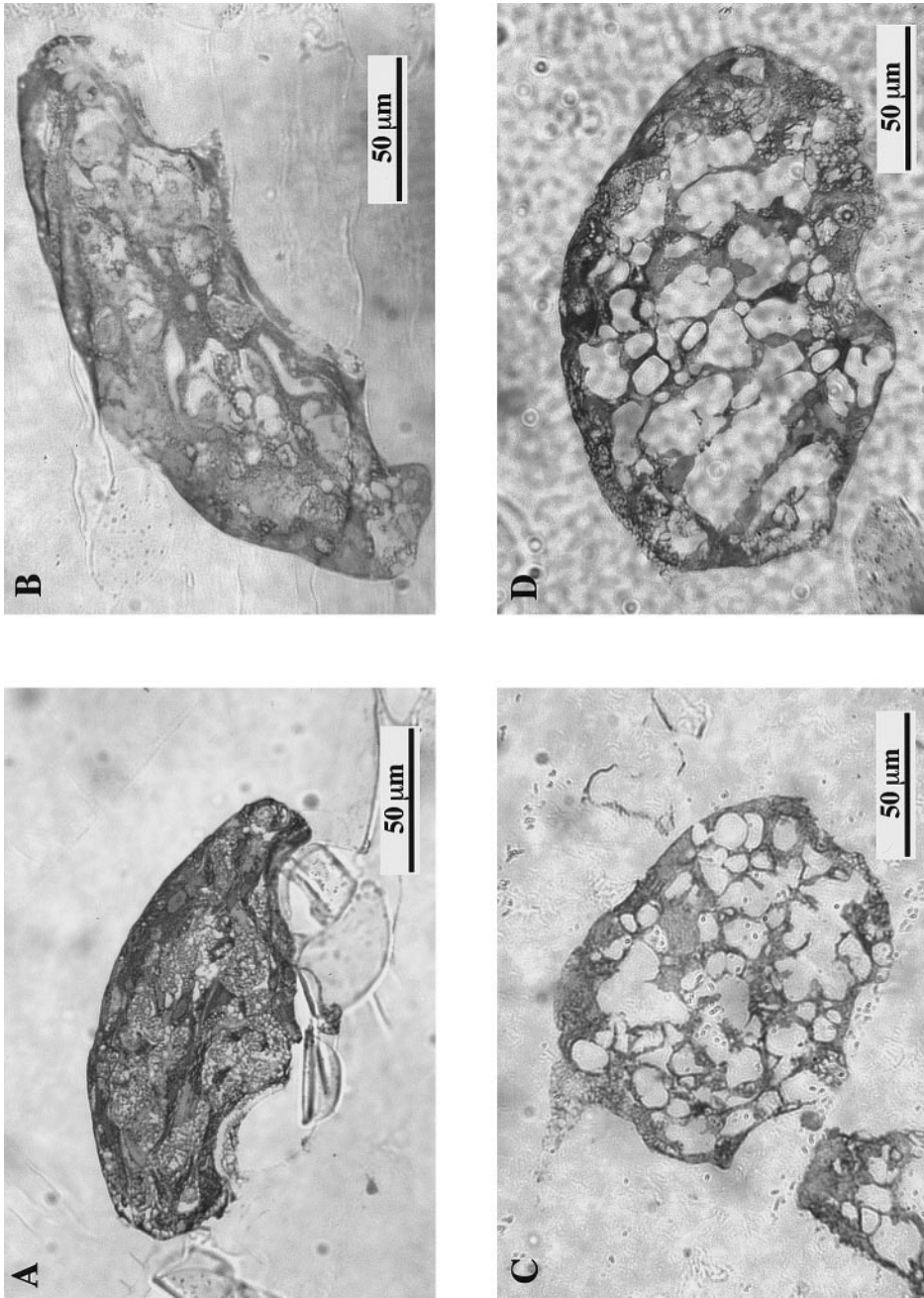


FIG. 5. Cross-sectional slices of hepatocyte spheroids at different final temperatures. The spheroids were frozen in William's E medium at a cooling rate of $1^{\circ}\text{C}/\text{min}$ and a final temperature of (A) -3°C ; (B) -5°C ; (C) -12°C ; (D) -16°C .

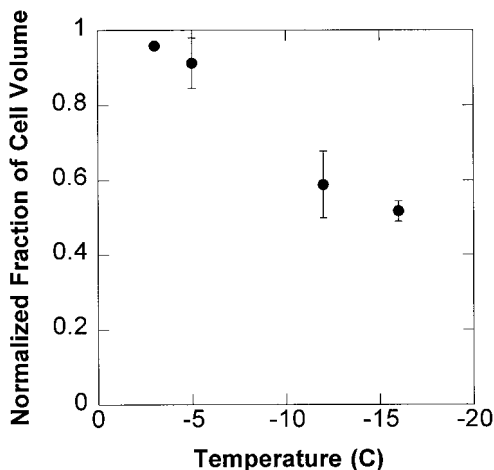


FIG. 6. Normalized fraction of cells in the spheroid as a function of temperature, cooled at 1°C/min. The fraction of cells is obtained by assuming that the ratio cellular area to spheroid area is uniform throughout the volume of the spheroid and normalizing this ratio over the control samples that were plunger-frozen from room temperature.

oid during freezing. For rapidly cooled samples (100°C/min) ice crystals of diameters of 10 μm or less were observed throughout the cells of the spheroid. Although it was difficult to determine the precise location of cell and nuclear membranes, the ice crystals appeared to be located in both cytoplasmic and nuclear regions. The size and distribution of ice crystals observed in this investigation are consistent with those observed in previous studies of rapidly frozen liver tissue (2).

The method for calculating the normalized cell volume fraction used in Fig. 6 relied on the assumption that the overall spheroid volume does not change significantly during freezing. In addition, it was assumed that the cross-sectional area of the spheroid (at any depth) stays the same with decreasing temperature. These assumptions introduce error into the calculation of normalized cell fraction in the spheroid during freezing. Previous cryomicroscopy studies have shown that the dehydration of the outer diameter of the spheroid is typically less than 14% (5).

An important element in understanding the osmotic response to spheroids during freezing at slower cooling rates requires knowledge of the distribution of ice crystals throughout the spheroid. The freeze-substituted sections obtained show the formation of large ice crystals in the central portion of the spheroid during freezing. The size of the ice crystals increases as the temperature decreases. It is not possible to state conclusively whether the ice observed is intra- or intercellular ice. The images shown in Fig. 5 show the growth of large ice crystals as the temperature decreases. The size of these crystals was larger than the size of a single cell. As a result, it is unlikely that the large ice crystals observed represent intracellular ice formation. The formation of large crystals in the extracellular ice may explain why the overall volume of the spheroid does not decrease during freezing. Measurements of the normalized cell

TABLE 2
Water Transport Parameters for Isolated Hepatocytes of Different Species

Species	$L_{pg}, \times 10^{13}$ (m^3/Ns)	E_{ip} (kJ/mol)	V_b	$\Omega_o, \times 10^{-8}$ ($\text{m}^{-2} \text{s}^{-1}$)	$\kappa_o, \times 10^{-9}$ (K^5)
Human ^a	1.6	216	0.23	7.6	0.75
Rat ^b	15	341	0.51	110	1.4
Rat cells digested from collagen sandwich ^b	0.63	238	ND ^c	237	0.33
Pig ^a	5.8	480	0.25	13	0.48
Disaggregated pig spheroid	0.076	82	0.32	5.9	3.0

^a Cf. Ref. (6).

^b Cf. Refs. (37, 34).

^c Not determined.

volume fraction indicate extensive dehydration of cells in the spheroid. The ubiquitous distribution of the ice crystals also implies that ice formation in the extracellular space is not limited to the bile-cannaliculi-like channels found in the spheroid. In spite of the extensive ice formation in the extracellular space, freeze-substituted sections show evidence of cell-to-cell contact in the spheroid even after extensive dehydration. Little or no ice crystals are observed in the outer layer(s) of cells in the spheroid.

SUMMARY

The pig hepatocyte spheroids exhibit transport characteristics that are distinct from those of isolated cells. The spheroids dehydrate in hypertonic solutions, but less than might be expected from the dehydration of freshly isolated pig hepatocytes. The disaggregation of the cultured spheroids and subsequent cryomicroscope analysis shows a decrease in water permeability parameters and changes in the intracellular ice formation coefficients consistent with previous studies. During slow cooling, large ice crystals are observed in the interior of the spheroid and these crystals most probably form in the extracellular space. Rapidly cooled spheroids exhibit small but visible ice crystals distributed in the nuclear and cytoplasmic regions.

ACKNOWLEDGMENTS

This work is supported in part by a grant from the National Institutes of Health (GM-54886). B.K. was supported by a NSF Training Grant (BIR-9413241). Special thanks are given to Rory Rimmel and W. S. Hu for hepatocytes and John Bischof, Paul Barrat, David Smith, and Chris Frethem for help with the techniques of freeze substitution and ultramicrotome sectioning.

REFERENCES

1. Barcellos-Hoff, M. H., Aggler, J., Ram, T. G., and Bissel, M. J. Functional differentiation and alveolar morphogenesis of primary mammary cultures on reconstituted basement membrane. *Development* **105**, 223–235 (1989).
2. Bischof, J. C., and Rubinsky, B. Large ice crystals in the nucleus of rapidly frozen liver cells. *Cryobiology* **30**, 597–603 (1993).
3. Casciari, J. J., Sotircos, S. V., and Sutherland, R. M. Glucose diffusivity in multicellular tumor spheroids. *Cancer Res.* **48**, 3905–3909 (1988).
4. Cosman, M., Toner, M., Kandel, J., and Cravalho, E. An integrated cryomicroscopy system. *Cryo-Lett.* **10**, 17–38 (1989).
5. Darr, T. B., and Hubel, A. Investigation of subzero water transport properties for isolated hepatocytes and hepatocytes cultured in spheroids. *ASME Biomed. Eng.* **BED-29**, 269–270 (1995).
6. Darr, T. B., and Hubel, A. Freezing characteristics of isolated pig and human hepatocytes. *Cell Transplant.* **6**(2), 173–183 (1997).
7. Devireddy, R. V., and Bischof, J. C. Measurement of water transport during freezing in mammalian liver tissue. II. The use of differential scanning calorimetry. *J. Biomech. Eng.* **120**(5), 559–569 (1998).
8. de Freitas, R. C., Diller, K. R., Lakey, J. R. T., and Rajotte, R. V. Osmotic behavior and transport properties of human islets in a dimethyl sulfoxide solution. *Cryobiology* **35**(3), 230–239 (1997).
9. Freyer, J. P., and R. M. Sutherland. Regulation of growth saturation and development of necrosis in EMT6/R multicellular spheroids by the oxygen and glucose supply. *Cancer Res.* **46**, 3504–3512 (1986).
10. Halban, P. A., Powers, S. L., George, S. L., and Bonner-Weir S. Spontaneous reassociation of dispersed adult rat pancreatic islets cells into aggregates with three-dimensional architecture typical of native islets. *Diabetes* **36**, 783–790 (1987).
11. Hubel, A., Cravalho, E. G., Nunner, B., and Korber, Ch. Survival of directionally solidified B-lymphoblasts under various crystal growth conditions. *Cryobiology* **29**, 183–198 (1992).
12. Karlsson, J., Cravalho, E., Rinkes, I., Tompkins, R., Yarmush, M., and Toner, M. Nucleation and growth of ice crystals inside cultured hepatocytes during freezing in the presence of dimethyl sulfoxide. *Biophys. J.* **65**, 2524–2534 (1993).
13. Koide, N., Shinji, T., Tanabe, T., Asano, K., Kawaguchi, M., Sakaguchi, K., Koide, Y., Mori, M., and Tsuji, T. Continued high albumin production by multicellular spheroids of adult rat hepatocytes formed in the presence of liver-derived proteoglycans. *Biochem. Biophys. Res. Commun.* **161**, 385–391 (1989).
14. Korniski, B., and Hubel, A. A model of low-temperature water transport for hematocyte spheroids. *Ann. N. Y. Acad. Sci.* **858**, 183–190 (1998).
15. Lazar, A., Peshwa, M. V., Wu, F. J., Chi, C. M., Cerra, F. B., and Hu, W. S. Formation of porcine hepatocyte spheroids for use in bioartificial liver. *Cell Transplant.* **4**(3), 259–268 (1995).
16. Lazar, A., Mann, H. J., Rimmel, R. P., Sharford, R. P., Cerra, f. B., and Hu, W. S. Extended liver-specific function of porcine hepatocyte spheroids entrapped

- in collagen gel. *In Vitro Cell. Dev. Biol.* **31**(5), 340–346 (1995).
17. Levin, R. L., Cravalho, E. G., and Huggins, C. E. A membrane model describing the effect of temperature on the water conductivity of erythrocyte membranes at subzero temperatures. *Cryobiology* **13**, 415–429 (1976).
 18. Lovelock, J. E. The haemolysis of human red blood cells by freezing and thawing. *Biochem. Biophys. Acta* **10**, 414–426 (1953).
 19. Mazur, P. Kinetics of water loss from cells at subzero temperatures and the likelihood of intracellular freezing. *J. Gen. Physiol.* **47**, 347–369 (1963).
 20. Mazur, P. Freezing of living cells: Mechanisms and implications. *Am. J. Physiol.* **247**, C125–C142 (1984).
 21. Merchant, F. A., Aggarwal, S. J., Diller, K. R., Bartels, K. A., and Bovik, A. C. Analysis of volumetric changes in rat pancreatic islets under osmotic stress using laser scanning confocal microscopy. *Biomed. Sci. Instrument.* **29**, 111–119 (1993).
 22. Pazhayannur, P. V., and Bischof, J. C. Measurement and simulation of water transport during freezing in mammalian liver tissue. *J. Biomech. Eng.* **119**(3), 269–277 (1997).
 23. Pegg, D. E., and Diaper, M. P. On the mechanism of injury to slowly frozen erythrocytes. *Biophys. J.* **54**, 471–488 (1988).
 24. Peshwa, M. V., Wu, F. J., Follstad, B. D., Cerra, F. B., and Hu, W. S. Kinetics of hepatocyte spheroid formation. *Biotechnol. Prog.* **10**, 460–466 (1994).
 25. Peshwa, M. V., Wu, F. J., Sharp, H. L., Cerra, F. B., and Hu, W. S. Mechanistics of formation and ultrastructural evaluation of hepatocyte spheroids. *In Vitro Cell. Dev.* **32**(4), 197–203 (1996).
 26. Robards, A. W., and Sleytr, U. B. "Practical Methods in Electron Microscopy," Vol. 10, Chapters 2 and 7, Elsevier, Amsterdam, 1985.
 27. Rubinsky, B., and Pegg, D. E. A mathematical model for the freezing process in biological tissue. *Proc. R. Soc. Lond. B* **234**, 343–358 (1988).
 28. Sakai, Y., Naruse, K., Nagashima, I., Meito, T., and Suzuki, M. Y. Short-term hypothermic preservation of porcine hepatocyte spheroids using UW solution. *Cell Transplant.* **5**(4), 505–511 (1996).
 29. Seglen, P. O. Preparation of isolated rat liver cells. *Methods Cell Biol.* **13**, 29–38 (1976).
 30. Shannon, J. M., Mason, R. J., and Jennings, S. D. Functional differentiation of alveolar type II epithelial cells in vitro: Effects of cell shape, cell–matrix interactions and cell–cell interactions. *Biochim. Biophys. Acta* **931**, 143–156 (1987).
 31. Tobe, S., Takei, Y., Kobayashi, K., and Akaike, T. Receptor-mediated formation of multilayer aggregates of primary cultured adult rat hepatocytes on lactose-substituted polystyrene. *Biochem. Biophys. Res. Commun.* **184**, 225–230 (1992).
 32. Toner, M. Nucleation of ice crystals inside biological cells. In "Low-Temperature Biology" (P. Steponkus, Ed.), pp. 1–51, JAI Press, London, 1993.
 33. Toner, M., Cravalho, E., and Karel, M. Thermodynamics and kinetics of intracellular ice formation during freezing of biological cells. *J. Appl. Phys.* **67**(3), 1582–1593 (1990).
 34. Toner, M., Tompkins, R. G., Cravalho, E. G., and Yarmush, M. L. Transport phenomena during freezing of isolated hepatocytes. *AIChE J.* **38**(10), 1512–1522 (1992).
 35. Tong, J. Z., De, L. P., Furlan, V., Cresteil, T., Bernard, O., and Alvarez, F. Long-term culture of adult rat hepatocyte spheroids. *Exp. Cell Res.* **200**, 326–332 (1992).
 36. Wu, F. J., Friend, J. R., Hsaio, C. C., Zilliox, M. J., Ko, W. J., Cerra, F. B., and Hu, W. S. Efficient assembly of rat hepatocyte spheroids for tissue engineering applications. *Biotech. Bioeng.* **50**, 404–415 (1996).
 37. Yarmush, M. L., Toner, M., Dunn, J., Rotem, A., Hubel, A., and Tompkins, R. Hepatic tissue engineering: Development of critical technologies. *Ann. N. Y. Acad. Sci.* **665**, 238–252 (1992).